

Uncoupling lifespan and healthspan in *Caenorhabditis elegans* longevity mutants

 Ankita Bansal^a, Lihua J. Zhu^{a,b,c}, Kelvin Yen^{a,1}, and Heidi A. Tissenbaum^{a,c,2}

 Programs in ^aGene Function and Expression, ^bBioinformatics and Integrative Biology, and ^cMolecular Medicine, University of Massachusetts Medical School, Worcester, MA 01605

Edited* by Gary Ruvkun, Massachusetts General Hospital, Boston, MA, and approved November 21, 2014 (received for review June 27, 2014)

Aging research has been very successful at identifying signaling pathways and evolutionarily conserved genes that extend lifespan with the assumption that an increase in lifespan will also increase healthspan. However, it is largely unknown whether we are extending the healthy time of life or simply prolonging a period of frailty with increased incidence of age-associated diseases. Here we use *Caenorhabditis elegans*, one of the premiere systems for lifespan studies, to determine whether lifespan and healthspan are intrinsically correlated. We conducted multiple cellular and organismal assays on wild type as well as four long-lived mutants (insulin/insulin-like growth factor-1, dietary restriction, protein translation, mitochondrial signaling) in a longitudinal manner to determine the health of the animals as they age. We find that some long-lived mutants performed better than wild type when measured chronologically (number of days). However, all long-lived mutants increased the proportion of time spent in a frail state. Together, these data suggest that lifespan can no longer be the sole parameter of interest and reveal the importance of evaluating multiple healthspan parameters for future studies on antiaging interventions.

healthspan | lifespan | gerospan | functional capacity | healthy aging

Advances in technology, healthcare, and nutrition have considerably increased the average life expectancy worldwide. In addition, lower birthrates in developed countries along with a decline in the adult mortality rate have led to an increase in the number of older individuals worldwide. According to the World Health Organization, the population of people living 85 y and beyond is predicted to increase by 351% globally in the next 40 y (1). Because aging is accompanied by an increased incidence of many diseases including cancer, arthritis, obesity, and diabetes, the majority of healthcare costs are associated with the last few years of life, which could lead to an economic disaster (2). One possible solution could involve aging research focused on increasing the health of the aging population (3).

Over the last two decades, aging research has focused on lifespan regulation with little attention to the health of the animal. Studies with model systems such as yeast, worms, and flies have identified hundreds of different genes, regimens, and chemicals that modulate lifespan. Many of these life-extending treatments are also conserved in mammals (4, 5). In the nematode *Caenorhabditis elegans* (*C. elegans*), multiple pathways including insulin/insulin-like growth factor (IGF)-1 signaling, dietary restriction, altering mitochondrial signaling, and protein translation modulate mean and maximal lifespan (6–11). Lifespan has been considered the ultimate parameter, defined as the period an organism survives. The common assumption that treatments, which increase lifespan, would prolong health or healthspan is supported by previous studies that suggest a correlation between increased stress resistance and lifespan extension (12–17). However, these studies have been limited by only testing animals at younger ages; older animals have rarely been examined.

In *C. elegans*, age-associated phenotypes such as changes in movement capacity have had conflicting results about whether movement decline correlates with lifespan (18, 19). Another se-

ries of *C. elegans* studies suggests that some life-extending treatments improve cognitive function, including performance and memory function, whereas others do not (20, 21). In *Drosophila*, dietary-restricted flies show lifespan extension but no improvement in their cognitive ability (aversion learning test) compared with wild type (22). In another study, dietary restriction did not provide functional benefits to older flies (23). Finally, flies exposed to different concentrations of the anticonvulsant lamotrigine, known to increase the lifespan of worms, reduced movement capacity significantly as the flies aged, suggesting that lifespan extension led to an increase in frailty (24). Together, these data show the importance of further dissecting the connection between lifespan and healthspan.

Although the term lifespan is well-defined, there is no single, generally accepted definition of health or healthspan. In a clinical setting, the term most commonly used to predict age-related mortality is the frailty index (FI). FI is defined per individual as the proportion of deficits present out of the total number of age-related health variables, which broadly covers self-sufficiency and disease-free state in human beings (25, 26). In the laboratory, as mentioned above, several studies have examined physiological changes with age (19, 27, 28). The term healthspan is poorly defined and, in *C. elegans*, few parameters such as movement, pharyngeal pumping (feeding), and lipofuscin accumulation (29–33) have been measured as healthspan parameters as the animals age. There has yet to be a comprehensive definition of healthspan in the laboratory.

Significance

Genetic and environmental manipulations have been identified that result in lifespan extension. The underlying assumption that lifespan extension would also result in an increase in healthspan is seemingly valid but infrequently examined. Here, we examined multiple pathways that modulate lifespan to investigate the relationship between lifespan extension and health. We analyzed wild-type and four long-lived mutants in an unbiased cross-sectional study with multiple assays until animals reached 80% maximum lifespan. We show lifespan and healthspan can be separated and all of the long-lived mutants extend the period of frailty as a consequence. If applied to humans, this would likely lead to unsustainable healthcare costs and demonstrates the importance of examining healthspan as opposed to lifespan for future research.

Author contributions: A.B., K.Y., and H.A.T. designed research; A.B. performed research; A.B., L.J.Z., and H.A.T. contributed new reagents/analytic tools; A.B., L.J.Z., and H.A.T. analyzed data; and A.B. and H.A.T. wrote the paper.

The authors declare no conflict of interest.

*This Direct Submission article had a prearranged editor.

¹Present address: Davis School of Gerontology, University of Southern California, Los Angeles, CA 90089.

²To whom correspondence should be addressed. Email: heidi.tissenbaum@umassmed.edu.

This article contains supporting information online at www.pnas.org/lookup/suppl/doi:10.1073/pnas.1412192112/-DCSupplemental.

Here we broadly define healthspan by measuring multiple physiological parameters over the life of the worm (*SI Appendix, Fig. S1*). Our healthspan study has many important aspects, which include that (i) we measured healthspan using a large number of assays, (ii) we tested animals in multiple assays until ~80% of the population had died, and (iii) we calculated and compared the health of the different strains in two different ways: chronological (actual day) and physiological (as a percentage of maximal lifespan: allowing the determination of the percentage of healthy and frail periods of the entire lifespan of the animal). Taken together, our healthspan assays cover an FI as well as additional assays, including the ability to maintain homeostasis in response to external stress, movement, lipofuscin accumulation and feeding (pharyngeal pumping), and other cellular changes (*SI Appendix, Fig. S1B*).

Results

We tested four different long-lived mutants in this study, *daf-2(e1370)*, *eat-2(ad1113)*, *ife-2(ok306)*, and *clk-1(qm30)* [*daf*, abnormal dauer formation; *eat*, abnormal pharyngeal pumping; *ife*, initiation factor 4E (eIF4E) family; *clk*, (biological timing) abnormality], where each represent a different signaling pathway (insulin/IGF-1 signaling, dietary restriction, protein translation and mitochondrial signaling respectively) implicated in lifespan regulation. Fig. 1 shows lifespan analysis for all four mutants compared with wild type. All of the mutations result in increased mean and maximal lifespan compared with wild type (Fig. 1 and

SI Appendix, Fig. S2). *daf-2(e1370)* mutants, the canonical allele most routinely used, bear a mutation in the insulin/IGF-1 receptor that results in a doubling of lifespan (maximal lifespan of 57 d compared with 30 d for wild type) (6).

Dietary restriction is an environmental intervention proven to increase lifespan in animals ranging from yeast to mammals (34–36). In *C. elegans*, at least seven different methods have been standardized to induce dietary restriction (37). Here we use the genetic model of dietary restriction in worms, *eat-2*, which has a maximal lifespan of 36 d, resulting in a 20% increase in lifespan compared with wild type (Fig. 1). These mutants have reduced feeding capacity due to a defective protein encoding the nicotinic acetylcholine receptor subunit that functions in the pharyngeal muscle to regulate the rate of pharyngeal pumping (38). Therefore, *eat* mutants have reduced food uptake, serving as a model of dietary restriction.

In *C. elegans*, modulating mitochondrial activity by the mutation of genes involved in electron transport chain activity is also known to increase lifespan. One of the genes, *clk-1*, results in mean and maximum lifespan extension in worms of 25% and 10%, respectively (Fig. 1) (8). The *clk-1* gene encodes an enzyme (demeoxyubiquinone monooxygenase) necessary for ubiquinone biosynthesis required during respiration for shuttling electrons from complex I and II to complex III (39). A heterozygous knockout of *mclk-1* in mice, the mammalian homolog of *C. elegans clk-1*, has reduced reactive oxygen species (ROS) levels, decreased ROS sensitivity, and ROS damage along with increased lifespan (39).

The fourth signaling cascade that modulates longevity in invertebrate models is the regulation of translation in the somatic tissues (9–11). These regulators include kinases that signal to promote mRNA translation, translation initiation factors, structural components of the ribosome, and ribosomal RNA processing factors. The eukaryotic initiation factor 4E (eIF4E) is a key modulator of protein translation because eIF4E binds the 7-monomethylguanosine cap at the 5' end of nuclear mRNAs (40). To serve as a model for protein translation, we used the gene *ife-2*. Knockdown of *ife-2*, the *C. elegans* isoform of eIF4E, increases maximal lifespan to 42 d compared with 30 d in wild type (Fig. 1) (9). In mice, inhibition of mammalian target of rapamycin, a key regulator of mRNA translation in response to nutrients, can also result in lifespan extension (41). In this study, we measured the health of different long-lived mutants to determine whether a meaningful increase in lifespan also translates into improved healthspan.

Next, the mortality curves from Fig. 1A were modeled with the commonly used Gompertz equation following the analysis of Yen et al. (42). Gompertz analysis is based on the observation that the mortality rate increases exponentially with time after middle age. It is represented by the equation $S = Ae^{Gt}$, where S is the mortality rate, A is the initial mortality rate calculated from the mortality rate before the exponential increase in deaths with age in a population, and G is the exponential (Gompertz) mortality rate coefficient.

The Gompertz variable is used to determine the rate of aging based on the calculation of the mortality rate doubling time (MRDT) given by $MRDT = 0.693/G$. For example, if a population of worms has an MRDT of 10 d, it signifies that the chance of those worms dying after sexual maturity doubles approximately every 10 d. Therefore, a lower value of G would indicate a higher MRDT and a slower rate of aging. Our data reveal that, compared with wild type, both *daf-2* and *clk-1* mutants had significant decreases in initial mortality rate and *daf-2*, *eat-2*, and *ife-2* had a significant decrease in the Gompertz variable as determined by the likelihood ratio test (Table 1). In terms of the aging rate, *daf-2*, *eat-2*, and *ife-2* decrease the value of the Gompertz variable, thereby reducing MRDT.

Because the Gompertz analysis only compares survival data, the rate of aging defined by this equation is limited; it gives no information on the health changes of the aging animal. Therefore, we

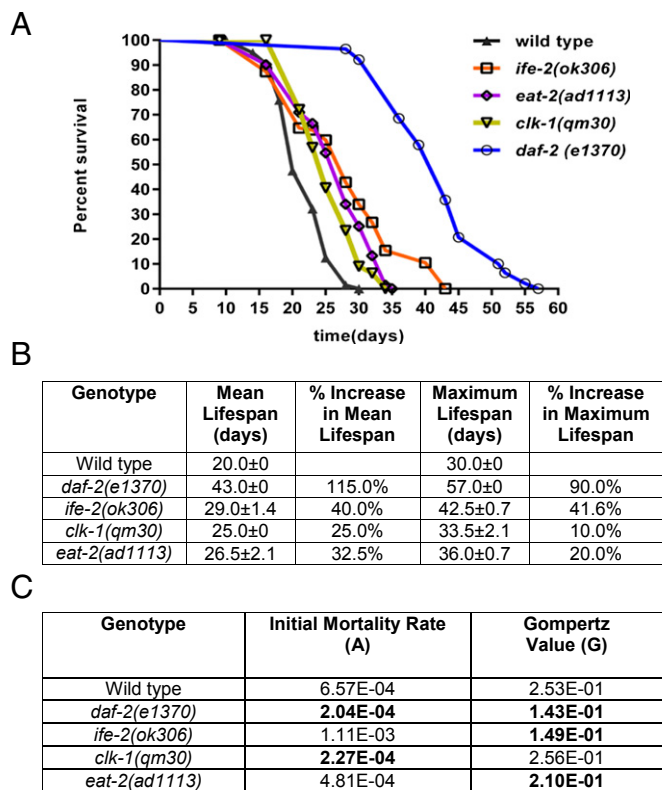


Fig. 1. Survival analysis of the strains used in the study. (A) Survival curve of all strains used in this study: wild type (black), *daf-2(e1370)* (blue), *eat-2(ad1113)* (purple), *ife-2(ok306)* (orange), and *clk-1(qm30)* (yellow). (B) All strains have different mean and maximal lifespan and show differences compared with wild type. (C) Gompertz analysis based on the mortality rate of the mutant strains compared with wild type. A, initial mortality rate; G, Gompertz variable. The values were derived from the survival curves. A lower G value indicates a slower aging rate.

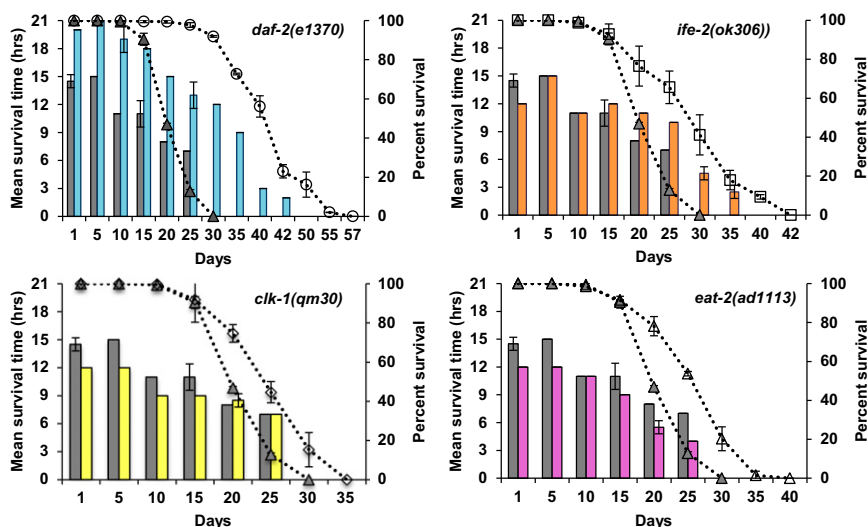


Fig. 2. Resistance to heat stress decreases with age. Each graph represents a different long-lived mutant compared with wild type. The bar graph shows the average of the mean survival time under heat stress for a population of aging animals for two biological repeats, plotted on the primary (left) y axis. The dotted lines represent the percent survival of the individual strains (lifespan analysis), plotted on the secondary (right) y axis. Wild type is shown in each graph as gray bars and gray triangles. (Upper Left) *daf-2(1370)*, blue bars and open circles. (Upper Right) *ife-2(ok306)*, orange bars and open squares. (Lower Left) *clk-1(qm30)*, yellow bars and open diamonds. (Lower Right) *eat-2(ad1113)*, pink bars and open triangles. For all strains, resistance to heat was measured for different ages of each strain until 80% of the animals were dead and declines with age. At day 1, compared with wild type, *clk-1*, *ife-2*, and *eat-2* mutants were sensitive to heat stress whereas *daf-2* mutants were resistant. Compared with wild type, when analyzed chronologically, *clk-1*, *ife-2*, and *daf-2* mutants show a similar rate of decline whereas *eat-2* mutants show a faster rate of decline in oxidative stress resistance capacity. Compared with wild type, when analyzed physiologically, *clk-1* and *eat-2* mutants show a faster rate of decline whereas *ife-2* and *daf-2* mutants show a similar rate of decline in heat stress resistance capacity (see text for additional details). Error bars represent SE from two biological repeats.

examined the health of wild type as well as different long-lived mutants by testing multiple parameters as the animals age. We then determined whether the rate of change in the different health parameters correlated with the prediction of the rate of aging based on the mortality curves.

Changes in Capacity to Maintain Homeostasis with Age. Aging involves the systemic loss of ability to recover from internal and external stresses in older people (43). We reasoned that healthy aged animals should have the ability to maintain homeostasis, which is defined as the ability to respond to physiological perturbations.

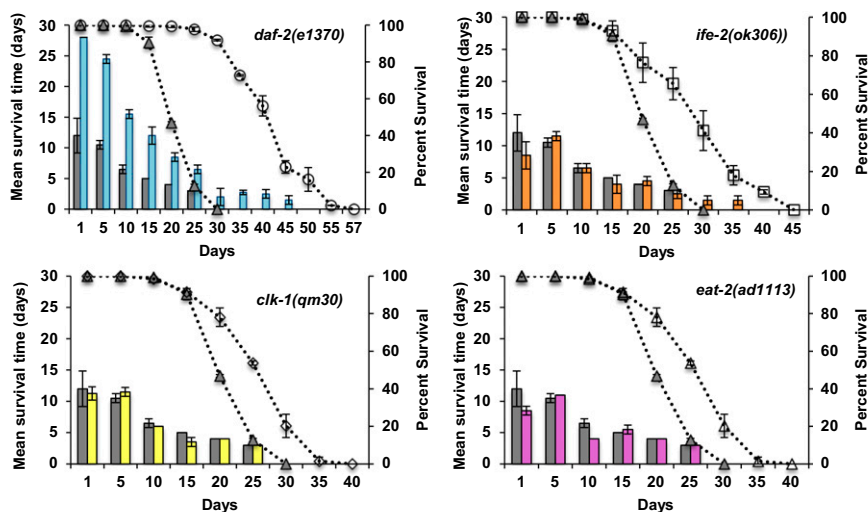


Fig. 3. Resistance to oxidative stress decreases with age. Each graph represents a different long-lived mutant compared with wild type. The bar graph shows the average of the mean survival time under oxidative stress for a population of aging animals for two biological repeats, plotted on the primary (left) y axis. The dotted lines represent the percent survival of the individual strains (lifespan analysis), plotted on the secondary (right) y axis. Wild type is shown in each graph as gray bars and gray triangles. (Upper Left) *daf-2(1370)*, blue bars and open circles. (Upper Right) *ife-2(ok306)*, orange bars and open squares. (Lower Left) *clk-1(qm30)*, yellow bars and open diamonds. (Lower Right) *eat-2(ad1113)*, pink bars and open triangles. For all strains, oxidative stress resistance was measured for different ages of each strain until 80% of the animals were dead and declines with age. Compared with wild type chronologically, *daf-2* mutants are more resistant to oxidative stress whereas *ife-2* and *clk-1* mutants are more sensitive to oxidative stress. Chronologically, compared with wild type, *eat-2*, *ife-2*, and *daf-2* mutants show a similar rate of decline whereas *clk-1* mutants have a slower rate of decline in oxidative stress resistance. Compared with wild type physiologically (age-matched population), *ife-2* and *clk-1* mutants show a similar rate of decline whereas *daf-2* and *eat-2* mutants show a faster rate of decline in oxidative stress resistance capacity (see text for additional details). Error bars represent SE from two biological repeats.

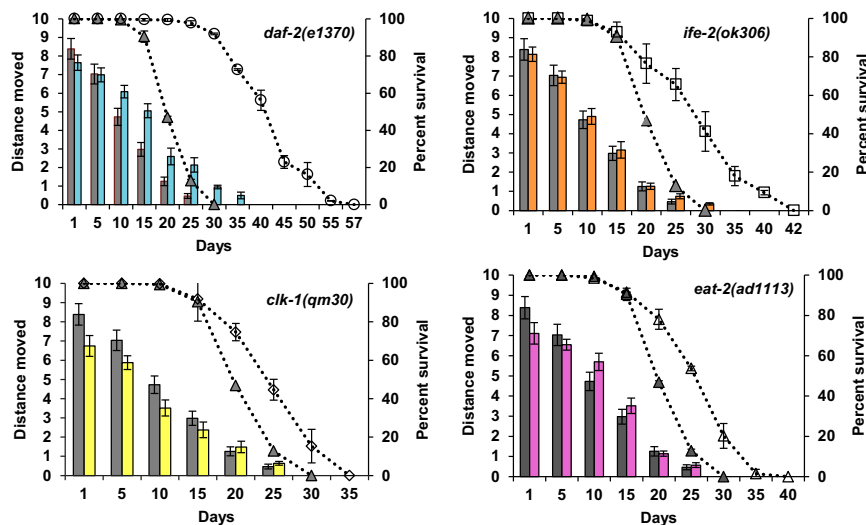


Fig. 4. Movement capacity of worms: distance traveled on solid media. Each graph represents a different long-lived mutant compared with wild type. The bar graph shows the average distance traveled on solid media plates for each age plotted on the primary (left) y axis. An average of 15 worms was singled onto seeded NGM plates and allowed to move for 5 min. The distance traveled was measured (arbitrary units) and compared with wild type (gray filled bars). The dotted lines represent the percent survival of the individual strains (lifespan analysis), plotted on the secondary (right) y axis compared with wild type (gray triangles). Each graph represents a different long-lived mutant compared with wild type (gray bars and gray triangles). (Upper Left) *daf-2(1370)*, blue bars and open circles. (Upper Right) *ife-2(ok306)*, orange bars and open squares. (Lower Left) *clk-1(qm30)*, yellow bars and open diamonds. (Lower Right) *eat-2(ad1113)*, pink bars and open triangles. For all strains, the distance moved was measured for different ages of each strain until 80% of the animals were dead and declines with age. Compared with wild type, at day 1, *eat-2* mutants cover significantly less distance whereas *clk-1*, *daf-2*, and *ife-2* mutants move a similar distance. Chronologically, compared with wild type, *daf-2* mutants' movement capacity (distance) declined at the same rate, *clk-1* and *ife-2* mutants lost their movement capacity at a slower rate, and *eat-2* mutants had a faster rate of decline. Physiologically (age-matched populations), compared with wild type, *daf-2* and *clk-1* mutants declined at the same rate, whereas *ife-2* and *eat-2* mutants lost their movement capacity faster (see text for additional details).

Therefore, the first set of assays tested was the response to heat stress and oxidative stress. Because these assays were terminal, a representative set of aging animals was tested every fifth day. For

all of the assays, we tested wild type as well as the four long-lived mutants, namely *daf-2(e1370)*, *eat-2(ad1113)*, *ife-2(ok306)*, and *clk-1(qm30)*.

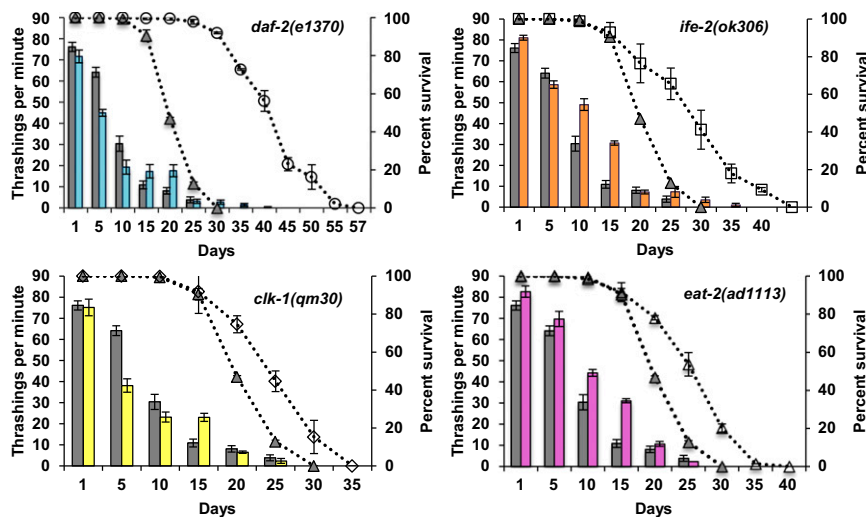


Fig. 5. Movement capacity of aging worms: movement in liquid media. Each graph represents a different long-lived mutant compared with wild type. The bar graph indicates the average thrashings per minute for each age (15 animals total) plotted on the primary (left) y axis. The worms were transferred to M9 media and allowed to move in the liquid. The number of thrashes per minute was counted and then plotted. The dotted lines represent the percent survival of the individual strains (lifespan analysis), plotted on the secondary (right) y axis compared with wild type (gray triangles). Each graph represents a different long-lived mutant compared with wild type (gray bars and gray triangles). (Upper Left) *daf-2(1370)*, blue bars and open circles. (Upper Right) *ife-2(ok306)*, orange bars and open squares. (Lower Left) *clk-1(qm30)*, yellow bars and open diamonds. (Lower Right) *eat-2(ad1113)*, pink bars and open triangles. For all strains, movement was measured for different ages of each strain until 80% of the animals were dead and declines with age. Compared with wild type chronologically, *daf-2* mutants thrash significantly less initially whereas *clk-1* mutants move similar to wild type. The rate of decline in thrashing capacity is faster than wild type until young/midlife and then slows down at older age. When compared chronologically to wild type, the rate of decline is higher for *eat-2* mutants and slower for *ife-2* mutants. Compared with wild type physiologically, *daf-2*, *clk-1*, and *eat-2* mutants show a faster rate of decline in movement capacity whereas for *ife-2* mutants, movement capacity declines at the same rate.

Table 1. Summary of the rate of decline in different health parameters when compared physiologically or age-matched populations

Genotype	Heat stress resistance	Oxidative stress resistance	Distance moved	Thrashing in liquid
<i>daf-2</i>	>WT	>WT	=WT	>WT
<i>eat-2</i>	>WT	>WT	>WT	>WT
<i>ife-2</i>	>WT	=WT	>WT	=WT
<i>clk-1</i>	>WT	=WT	=WT	=WT

For heat stress, every fifth day, plates were transferred to 37 °C and the population was assayed for their response. Consistent with previous studies (44), young *daf-2* mutants were resistant to heat stress compared with wild type ($P < 1e-16$) (Fig. 2). However, at day 1, the other long-lived mutants—the dietary restriction mutant *eat-2* and the protein translation mutant *ife-2*—were sensitive to heat stress ($P < 0.05$), whereas *clk-1* showed similar survival under heat stress compared with wild type (Fig. 2).

For oxidative stress, worms were transferred onto plates containing paraquat and the survival time was recorded. Initially, *daf-2(e1370)* mutants were resistant to oxidative stress ($P < 1e-16$) compared with wild type, whereas the other long-lived mutants showed higher sensitivity to paraquat (Fig. 3). Expectedly, for all of the strains, as the animals aged, stress resistance declined ($P < 0.001$), indicated by the gradual decrease in mean survival time under either heat or oxidative stress conditions.

Changes in Movement Capacity with Age. Another hallmark of human aging is sarcopenia, whereby skeletal muscle shows degenerative loss of mass, quality, and strength with age (45). Several *C. elegans* studies have observed sarcopenia in aging worms (27, 46, 47). This is seen as a reduction in cell size, loss of myofibrils, an increase in disorganization, and loss of nicely packed parallel structures of the myofibrils in worms (27, 47). In addition, similar to humans, a common feature of aging worms is reduced muscle function and mobility (18, 47, 48). Therefore, to further define health, we examined the changes in the movement capacity of aging wild-type and long-lived animals.

We tested the ability of animals to move in two different ways: on solid media and in liquid media. For movement on solid media, we measured the distance traveled over a finite period, which has previously been suggested to correlate with lifespan (19). As expected and consistent with previous reports (18, 19, 27), the total distance traveled on solid media decreased with age for all of the strains ($P < 2e-16$) (Fig. 4). As shown in Fig. 4, *daf-2* mutants move better than wild type from day 10 to day 20, whereas the other long-lived mutants move similar to wild type. The second method to assess the movement ability of aging worms was movement in liquid media (also known as swimming or thrashing) calculated by the number of body bends for an individual animal per minute. This differs from movement on solid media, because the worms are forced to move and the lateral body movement or thrashing of the animal is counted. We video-recorded the animals in the liquid media and then counted the number of thrashes per minute. Similar to the other assays, for all mutants, the thrashing rate declined with age. Interestingly, the animals lost their ability to thrash much earlier than movement on solid media (Fig. 5). In addition, many animals showed an uncoordinated movement pattern (Movies S1–S5) that increased with age irrespective of genotype. It is possible that this phenotype is associated with altered neuronal signaling (27) or neuronal aging (49, 50), which also do not correlate with lifespan or changes in the neuromuscular junction (51).

Next, we examined whether the changes in movement capacity could be due to the loss of muscle fiber structure. Phalloidin binds to actin in muscle fibers, and therefore we used phalloidin staining

to examine the muscle structure of the aging animals (52). Worms were grown and collected at four different time points (day 1, 5, 10, 15) and then fixed and stained with phalloidin (SI Appendix, Fig. S3). SI Appendix, Fig. S3 shows an example of the phalloidin staining for all strains at day 15. All of the animals show visible signs of muscle degradation, as evidenced by a reduction in muscle cell size, loss of parallel fibers, and increased disorganization. Then, we examined whether this muscle degradation correlated with lifespan as previously suggested (27). However, similar to our results in the movement assays, both wild type and the long-lived mutants showed similar signs of muscle fiber disorganization despite the differences in lifespan of these five strains: day 15 represents 50% maximal lifespan for wild type; 26% maximal lifespan for *daf-2*; 40% maximal lifespan for *eat-2*; 35% maximal lifespan for *ife-2*; and 44% maximal lifespan for *clk-1*. This suggests that the early loss of motility observed in the long-lived animals may be attributed to the collapse of the muscle fibers themselves.

To feed, worms use a neuromuscular organ called the pharynx that contracts, allowing food to be ingested and then ground for use as an energy source. The rate of pharyngeal contraction, also known as pharyngeal pumping, is regulated to adapt to the amount and quality of food (53). Pharyngeal pumping declines with age (19). It has been suggested that this is due to two major reasons: the increased growth of bacteria in the pharynx as the animals age that leads to bacterial plugging, and/or the decline in the structure due to constant muscle contractions and age-associated degeneration of muscle structure (19, 27). Therefore, previous studies have used pharyngeal pumping as a marker of healthspan in *C. elegans*. We recorded and counted the frequency of pharyngeal pumping every fifth day as the animals aged. However, after day 15, irrespective of the genotype, animals showed little or no pumping (Fig. 6). Because the objective of this study was to evaluate the effect of the life-extending mutations in older animals, pharyngeal pumping cannot be considered as a healthspan parameter. Our results also suggest that the long-lived animals do not provide protection from the age-related loss of pumping capacity. Similar to our results, Chow et al. (48) observed little or no pharyngeal pumping after day 12 of adulthood.

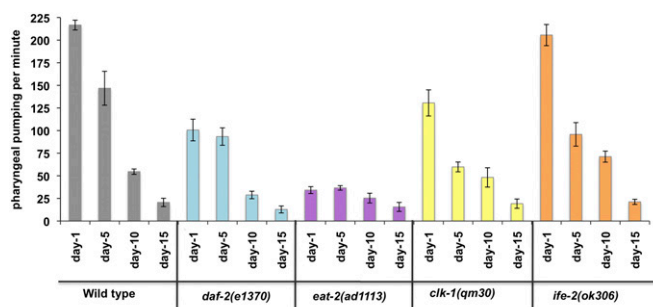


Fig. 6. Pharyngeal pumping of aging worms. The bars represent the number of pharyngeal contractions per minute. Pumping rate declines with age for all of the strains until day 15. After day 15, all strains show negligible pumping. Error bars represent the SE for each strain ($n = 10$).

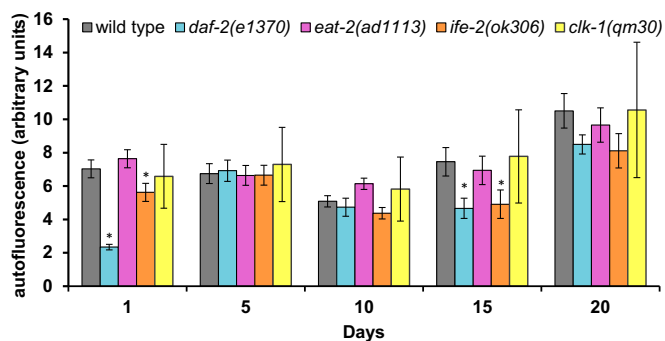


Fig. 7. Changes in autofluorescence with age (lipofuscin). The bar graph indicates the changes in autofluorescence as the worms age. The amount of autofluorescence increased in all of the mutants. Compared with wild type, both *daf-2* and *ife-2* mutants show significantly lower accumulation at day 1 and day 15. After day 20, regardless of their mean/maximal lifespan, all of the strains show similar amounts of lipofuscin accumulation. * $P < 0.05$.

Autofluorescence/Lipofuscin Accumulation. Another conserved phenomenon observed to change with age is the accumulation of the age-related fluorescent pigments or lipofuscin granules, which are the waste products that accumulate in the lysosomal cells (54). Even though the role of such pigments is unclear, lipofuscin visualization is often used as an age-related marker and a quantifier of healthspan in *C. elegans*. Therefore, we quantified this fluorescence with age (Fig. 7). Both long-lived mutants *daf-2* and *ife-2* showed significantly ($P < 0.05$) reduced age-associated granules compared with wild type at day 1 and day 15. However, after day 15, the amount of accumulated lipofuscin was not significantly different between any of the long-lived strains (Fig. 7). Given that all of the strains show different mean lifespan, these data suggest that although lipofuscin accumulation changes with age, the increased levels do not correlate with lifespan. Taken together, pharyngeal pumping and lipofuscin accumulation are age-related but not age-correlated because they are unaffected by the life-extending mutations, and should no longer be used as measures of healthspan.

Rate of Decline in Health Parameters with Age. Next, for each long-lived mutant, we computed the rate of decline in each healthspan parameter to determine the change in the functional capacity compared to wild type. A regression curve was fit to the values of different health parameters for all of the strains as they aged. Then, we compared the healthspan analysis with the rate of aging predicted by Gompertz analysis to see whether the lifespan analysis was sufficient to draw conclusions about the health changes observed in the aging animals (Tables 1 and 2 and *SI Appendix*, Tables S1–S12).

Statistical and model analysis of our healthspan data revealed that no single equation could account for more than one of the healthspan assays that were performed. This indicates that different cellular capacities deteriorate at distinct rates in aging worms. For a treatment or mutation to increase the healthy days,

the rate of decline in different parameters is expected to be slower than wild type. Our chronological data reveal that the rate of decline for the long-lived mutants was similar to wild type for stress resistance, except for *eat-2* mutants, which exhibit a faster rate of decline in all of the health parameters compared to wild type. None of the long-lived mutants tested slowed down the rate of decline in stress resistance capacity. In contrast, for movement compared with wild type chronologically, *daf-2*, *clk-1*, and *ife-2* slow down the rate of decline.

Next, we reasoned that because all strains exhibit different mean and maximal lifespan, it is important to evaluate healthspan if the strains are age-matched. Therefore, we reevaluated all of the healthspan data by normalizing them to the lifespan of wild type. This analysis is referred to as “physiological comparison.” Interestingly, none of the long-lived mutants slowed down the rate of decline in different health parameters when measured in an age-matched population. This indicates that even though proportional healthspan increase might be possible, the consequence would be a proportional increase in the frailty period. Notably, the decline in health status of the different mutant strains occurs much earlier than predicted by the Gompertz equation. Neither of the two variables in the Gompertz analysis (A or G) correlated with the decline in the health parameters tested. This indicated that the “rate of aging” as predicted by the Gompertz analysis is a measure similar to lifespan and not a good estimate of either the health of the population or of the individual animals. Taken together, when normalized for lifespan, all of the long-lived mutants have an increased frailty period. Therefore, any new method, intervention, or genetic alternation that alters healthspan should attempt to decrease the rate of decline physiologically.

Healthspan Versus Gerospan. To get an accurate assessment of the health of the animals, we suggest that the lifespan of an animal should be divided into two separate parts: healthspan and gerospan. Healthspan is defined as the period when the animal has greater than 50% of the maximal functional capacity of wild type. Gerospan is defined as the period when the animal has less than 50% of the maximal functional capacity of wild type. Ideally, a healthy long-lived mutant would exhibit an extension of healthspan and a compression of gerospan. Using these defined terms, we analyzed all of our healthspan data chronologically, simply counting the number of days spent in healthspan vs. gerospan for each mutant in each assay. Defining healthspan as a chronological function reveals that *daf-2* increases the number of healthy days in almost all of the parameters tested. However, the other long-lived mutants stayed healthy for a similar number of days as wild type (Fig. 8). Then, we calculated the gerospan illustrated by the brown bars (Fig. 8). This analysis reveals that irrespective of the genetic intervention, the gerospan or frailty period has been extended.

We then normalized the healthspan-to-gerospan ratio to their maximal lifespan (with the maximal lifespan set to 100%) and compared the different strains physiologically. As shown in Fig. 9, none of the long-lived mutants show a proportional increase in healthspan with a reduction in gerospan, indicating that in all

Table 2. Summary of the rate of decline in different health parameters when strains are compared chronologically

Genotype	Heat stress resistance	Oxidative stress resistance	Distance moved	Thrashing in liquid
<i>daf-2</i>	=WT	=WT	>WT initially <WT later	>WT initially <WT later
<i>eat-2</i>	<WT initially >WT later	=WT	>WT	>WT
<i>ife-2</i>	=WT	=WT	<WT	<WT
<i>clk-1</i>	<WT	<WT	<WT initially >WT later	>WT initially <WT later

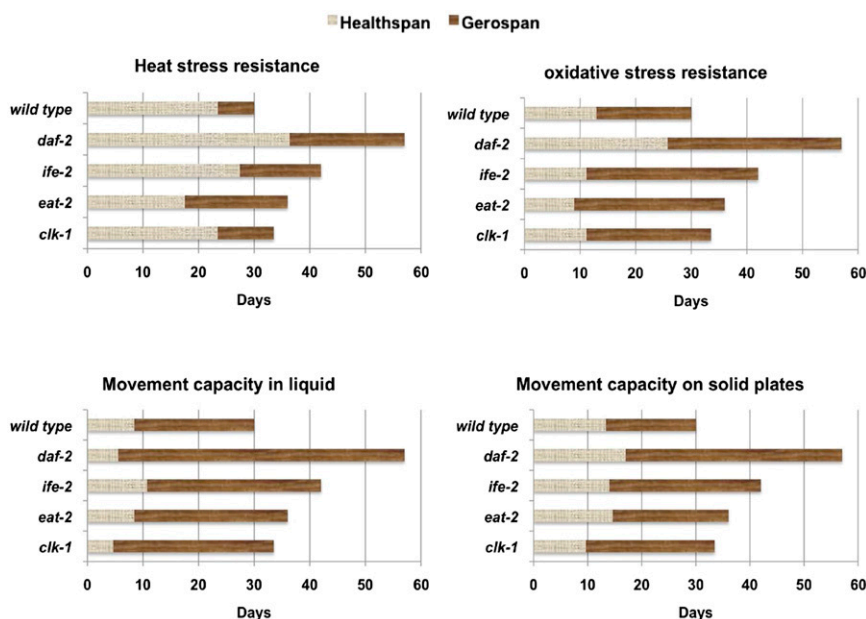


Fig. 8. Comparison of chronological healthspan vs. gerospan ratio. Healthspan is defined as the period when the animal has greater than 50% of the maximal functional capacity of wild type. Gerospan is defined as the period when the animal has less than 50% of the maximal functional capacity of wild type. Comparisons were made by comparing the results for each day and are based on the maximal number of days each strain survives.

cases lifespan extension does not proportionately increase healthspan. Therefore, these long-lived mutants add onto the frailty time rather than extending healthspan, indicating that there is a cost to extending the number of days an organism survives.

We have defined the terms healthspan and gerospan based on 50% of wild type functional capacity. Because this cutoff was arbitrarily defined, we decided to further explore these terms by setting the cutoff at a later time point: the ratio of healthspan to gerospan with a cutoff of 30% of wild-type functional capacity (or when the strains have lost 70% of their functional capacity compared with wild type) (*SI Appendix, Figs. S3–S5*). This, however,

gave a similar result to the 50% cutoff, indicating that none of the long-lived mutants result in an extension of healthspan along with compression of gerospan. Interestingly, when the gerospan cutoff was set to 30% of wild-type functional capacity, the healthiest animal is wild type (*SI Appendix, Fig. S5*). Taken together, our data suggest that defining healthspan and gerospan with 50% functional capacity of wild type is the best resolution of the data.

Discussion

Previously, the word “healthspan” has been used in many scientific contexts, but the definition has been ambiguous at best. Therefore,

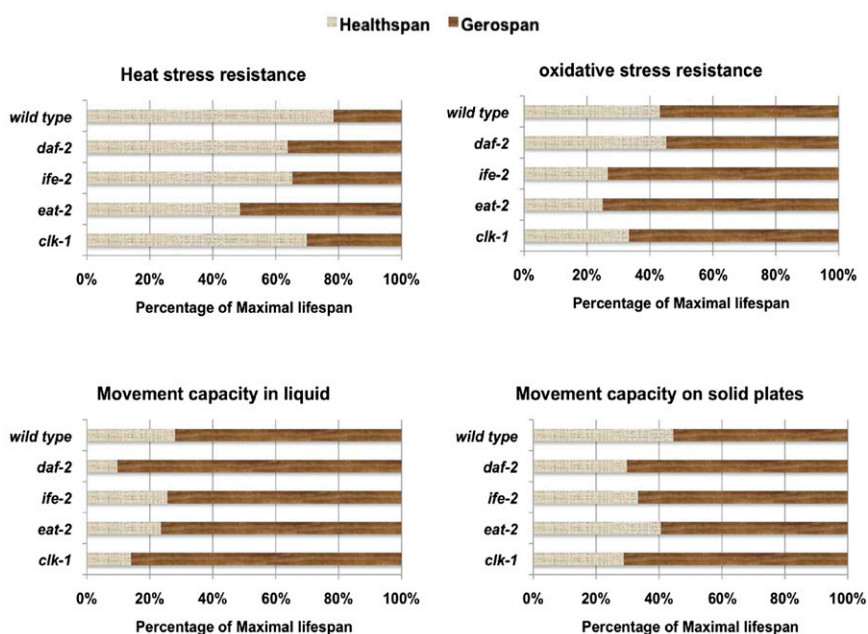


Fig. 9. Comparison of physiological healthspan vs. gerospan ratio. Comparisons were made by normalizing the maximal lifespan to 100% for all strains.

in this study, we focused on providing a conceptual framework of healthspan that can be easily verified in a laboratory setting using *C. elegans*. The current study makes no claim that the healthspan parameters tested cover all aspects of healthspan, nor does it make any assumptions that antiaging therapies that extend lifespan cannot coincide with an increase in healthspan. Rather, we highlight limitations of aging studies focused solely on lifespan extension.

Here we defined healthspan broadly by testing multiple assays as the animals aged. We tested wild type as our benchmark and then compared data from four long-lived mutants with wild-type health. From these data, we calculated and compared both the chronological number of days an animal is healthy vs. frail and the percent of the physiological lifespan the animal spends in each state (healthspan:gerospan ratio; Figs. 8 and 9).

Our data with the canonical allele of the *C. elegans* insulin/IGF-1 receptor homolog *daf-2(e1370)* reveals that, for multiple assays, these animals exhibit an increased number of healthy days. In addition, they increased the number of days spent in a frail state. When examining these data as a percentage of maximal lifespan, *daf-2* spends a larger proportion of life in a frail state than wild type (healthspan:gerospan ratio). Analyses of *eat-2* mutants, a genetic model for dietary restriction, as well as *clk-1* (mitochondrial mutant) show that both mutants extend lifespan but not healthspan when compared either chronologically or physiologically. In contrast, *ife-2* mutants, similar to *daf-2* mutants, increase the number of healthy days in some assays but spend a longer period of lifespan in a frail state as a consequence.

We also determined the rate of decline (dependent on each healthspan assay) for wild type as well as the four long-lived mutants. Our analysis revealed that depending on the health parameter tested (heat stress resistance, oxidative stress resistance, movement on plates, movement in liquid), in accordance with previous reports (27), each healthspan parameter declines with age at a different rate and this differs among the strains as well.

The rate of change in healthspan parameters with age was also compared with the rate of aging as calculated by the Gompertz variable. *daf-2*, *eat-2*, and *ife-2* mutants decrease the mortality rate as they age. However, our healthspan analysis suggests that this decline in the mortality rate does not equate to changes in health. Moreover, because the rate of mortality is reduced and the rate of decline in the health parameters is not, the long-lived mutants do not exhibit a proportional increase in healthspan. Rather, this results in an expansion of the frailty period or gerospan, when the data are normalized to maximal lifespan. Together, our data show that lifespan extension can result in an increased number of healthy days but that this will also increase the frailty period as a consequence, which ultimately would have disastrous economic and social consequences if applied to humans.

Thus far, the reports evaluating the healthspan of the four long-lived *C. elegans* mutants analyzed in this study have been limited. Gerstbrein et al. (29) used autofluorescent accumulation as a marker of healthspan and showed *daf-2(e1370)* mutants with lower levels of autofluorescent accumulation compared with wild type at day 12. Several other *C. elegans* studies have noted a vast number of age-related changes in wild type and some long-lived mutants (29). Liu et al. (51) examined changes in the neuromuscular junction in aging worms and found that two alleles of *daf-2* [*daf-2(e1368)* and *daf-2(1370)*] postponed the age-associated motor activity decline, with *daf-2(e1370)* showing a longer protective period. However, any comparisons have been chronological and few studies examined long-lived animals late into their maximum lifespan. Our study is the first attempt, to our knowledge, to measure both healthspan and gerospan as defined by the different measurements and calculate the period of each as a percentage of lifespan. Based on our analyses, we conclude that the mutants tested, at their best, are capable of maintaining a rate of decline in a health parameter similar to wild type. Although this means that a long-lived mutant can have a pro-

portionate increase in healthspan, there will also be an increase in the frailty period or gerospan as a result of the lifespan extension. Furthermore, resetting the gerospan threshold to 30% (i.e., when the animals have lost 70% of maximum wild-type capacity) suggests that wild type is the healthiest. In agreement with our results, genetic screens for healthspan mutants based on prolonged movement at advanced age have not identified any of the well-known long-lived mutants (31), indicating that the regulators of healthspan and lifespan thus far may be different.

Our results indicating that the increase in the absolute length of frailty in long-living mutants may be controversial, although perhaps not surprising. The antagonistic pleiotropic theory first proposed by Williams in 1957 states that aging is the result of the natural selection of many genes with pleiotropic function that benefit the young but will have an adverse effect later in life.

In agreement with this theory, it has been demonstrated by different groups that there is a fitness cost in the form of decreased fecundity as a result of extending lifespan in both worms and flies (55, 56). This indicates that healthspan has already been evolutionarily optimized and supports the idea that changes in lifespan do come at a measurable cost. Indeed, this has been found true for the long-lived mutants used in this study, where each mutant shows a reduced brood size at either normal or high temperature (57–60). In addition, given that the null phenotype of *daf-2* mutants is embryonic arrest (58), the healthspan results with *daf-2* may not be that unexpected.

It should be noted that we have only examined single mutants. Each of these strains has been backcrossed a limited number of times (*Materials and Methods*). It is still possible that any of these strains might bear mutations in the background that could contribute to a decrease in healthspan in any of the parameters tested. Indeed, it is also conceivable that altering multiple pathways could give rise to healthspan and lifespan extension. Arantes-Oliveira et al. (61) suggest that healthy long-lived animals arise from the combination of a mutation in *daf-2* (different allele from that used in this study) with *daf-2* RNAi and complete ablation of the germ line. Chen et al. (62) combined mutation in *daf-2* (similar allele to this study) with mutation in *rsk-1*, *C. elegans* S6 kinase to reveal extreme longevity. However, neither study analyzed the worms in multiple assays as they aged. Moreover, in both cases, there are drastic consequences of the lifespan extension: limited or no reproduction. It would be interesting, nonetheless, in future studies to test these combinations in a similar cross-sectional study.

The potential tradeoff due to increased lifespan may also extend to mammalian studies. Long-lived dietary-restricted and IGF-1-deficient mice show health deficits including delayed sexual maturity and reduced fertility along with reduced muscle strength (63, 64). In addition, dwarf mice eat normally, extend lifespan by 50%, but become obese and have muscle weakness in old age, which has an effect on their health. Unfortunately, this is often ignored because studies in mice often only sample early time points for comparison (reviewed in ref. 64).

With the older population increasing in numbers, non-communicable age-related diseases such as heart disease, cancer, and Alzheimer's disease are also on the rise (36). However, aging research has mainly focused on lifespan extension, with limited focus on determining whether this extension in lifespan comes at the cost of healthspan. Our data show that although we can increase lifespan and even healthspan in some assays, this also results in a disproportionate increase in gerospan or the time spent in a frail state. We suggest that, to improve the quality of life, the healthspan:gerospan ratio is much more informative than lifespan extension alone. Altogether, we suggest that to uncover genes and interventions that would result in healthy aging, research should shift the focus from lifespan extension to increasing healthspan and compressing gerospan.

Materials and Methods

Strain Maintenance. Worms were grown at 15 °C unless otherwise indicated on standard nematode growth medium (NGM) plates using standard *C. elegans* techniques (65). The following strains were used in this study: MQ130 *clk-1(qm30)* and KX15 *ife-2(ok306)*, both 10× backcrossed; DA1113 *eat-2(ad1113)*, 2× backcrossed; and CB1370 *daf-2(e1370)*, 5× backcrossed.

Lifespan Analysis. All strains were maintained at 15 °C. For each strain, gravid adults were isolated and then bleached to isolate eggs. Eggs were then placed in liquid overnight to obtain a synchronized population of L1 worms that were then plated and allowed to grow until they developed into young adults. Approximately 120 young adult worms were transferred onto four freshly seeded plates supplemented with 5-fluorodeoxyuridine (FuDR) to a final concentration of 0.1 mg/mL. These plates were then moved to a 20-°C incubator at day 1. Worms were scored by gently tapping with a platinum wire every 2–3 d. Worms that crawled off the plate, bagged, or died from vulval bursting were censored from the analysis. Statistical analyses for survival were conducted using the standard χ^2 -based log-rank test. Lifespan analysis was also repeated on non-FuDR plates (*SI Appendix, Fig. S2*), where animals were transferred to new plates every day for the first few days and then every 2–3 d after the worms had stopped laying eggs.

Healthspan Assays. All strains were maintained at 15 °C. For each strain, gravid adults were isolated and then bleached to isolate eggs. Eggs were then placed in liquid overnight to obtain a synchronized population of L1 worms that were then plated and allowed to grow until young adult worms. Approximately 1,200 young adult worms were picked onto 40 plates containing FuDR (0.1 mg/mL) and then shifted to 20 °C. Every fifth day, one plate of each strain was taken out for analysis (*SI Appendix, Fig. S1*). Each of the assays reported below has been repeated at least twice.

Resistance to Heat Stress. Every fifth day, one plate per strain was removed from 20 °C and transferred to 37 °C. Every 2 h, the worms were tapped with a platinum wire and worms that did not respond were scored as dead and counted. The percentage survival and mean survival was then calculated. Two biological repeats were done. Statistical analysis for survival was done using the standard χ^2 -based log-rank test.

Resistance to Oxidative Stress. One milliliter of paraquat solution (250 mM) was added onto the top of 30-mm plates. These plates were put on a shaker for 1 h and then placed in a laminar flow hood for 2 h to completely dry.

Approximately 30–40 worms were picked from the stock plates every fifth day at 20 °C onto paraquat plates. These plates were then put at 20 °C. Every 2 d, worms were tapped with a platinum wire to count the number of dead worms. The percentage survival was plotted and mean survival under oxidative stress was calculated. Two biological repeats were done. Statistical analyses for survival were conducted using the standard χ^2 -based log-rank test.

Locomotion Assays. On solid media plates, 15 worms were picked individually onto 15 freshly seeded 35-mm NGM plates. After 5 min, the worms were removed and a picture of the tracks made by the worms on the food was taken with a Nikon Coolpix 995 camera. The average distance covered was calculated by measuring the traces on the bacterial lawn using the software ImageJ (NIH).

In liquid, every fifth day, 13–15 worms were picked from the stock plates at 20 °C and transferred to 24-well plates containing 1 mL of M9 solution in each well. The worms were allowed to equilibrate for ~30 s, and then the thrashing was recorded using a Nikon Coolpix 995 camera. The average thrashings per minute were computed and then plotted for all of the strains.

Pharyngeal Pumping. Worms were observed under the Zeiss Stemi 2000 microscope with focus on the pharynx. Pharyngeal pumping was calculated for 30 s and then plotted.

Phalloidin Staining. Every fifth day, worms were washed off the plates with M9 buffer and collected into a microcentrifuge tube to pellet the worms. Phal-

loidin staining was performed using a modified protocol from Costa et al. (66). Briefly, worm pellets were washed twice with M9 buffer and then fixed using three freeze/thaw cycles in 2× modified Ruvkun's witches brew buffer as described in Yen et al. (67). Worms were then washed once with PBS and then once with 70% (vol/vol) methanol. Two units of fluorescein-conjugated phalloidin (Molecular Probes) was added and worm pellets were dried in a dark room for 2 h. Twenty microliters of 5 Mix (66) was then added to dissolve the phalloidin and left to stain at room temperature for 1 h. The worm pellet was then washed twice with PBS, 0.5% BSA, 0.5% Tween 20. The stained worms were mounted on slides and observed under a FITC filter using an Axioskop 2 Plus microscope.

Autofluorescence Measurement. Every fifth day, 10–15 worms were taken and mounted on a slide. Photos were then taken at 300-ms exposure under a DAPI filter using an Axioskop 2 Plus microscope. The fluorescence was calculated using ImageJ software.

Statistical Analysis. The log-rank test was used for comparing the survival curve of various mutants with wild type, and the mean survival time for each mutant at every fifth day was determined.

Statistical Methods for Calculation of the Rate of Decline in Stress Resistance.

For the first healthspan parameter, homeostatic response to stress (oxidative stress and heat stress experiment), a Cox proportional hazards model was fit to the survival data using the software R, software for statistical computation and graphics (68). This analysis was used for the following predictor variables: age, genotype, and the interaction between age (or normalized age by corresponding median lifespan) and genotype (68). In addition, we took the variability due to replicate experiments into account by adding a dummy variable in the model. From this model, the output is the hazard ratio (rate of hazards relative to wild type) for each mutant. For our healthspan studies, this ratio refers to the likelihood that the mutant will die from the stress at a given time compared with wild type. This model then incorporates different covariates (age and genotype) and predicts how the hazard ratio changes in response to the covariates age and genotype. Because the lifespan survival curve is non-linear, we used a forward selection method that could include with increasing order of the polynomial term for age and its interaction with genotype. Then, we used the partial likelihood ratio test and a χ^2 test to determine the best-fit model.

Statistical Methods for Calculation of the Rate of Decline in Movement Capacity.

Using R, a system for statistical computation and graphics, an ANOVA was performed to assess whether aging and genotype affect distance traveled and thrashing frequency, and whether an effect of aging differs among genotypes. A linear model was fit to include a randomized complete block design with an experiment as block effect, age, genotype, and the interaction between age and genotype. An *F* test was used to determine the best model fit that would take into account age, genotype, and their interaction.

Software Used in This Study. Statistical analyses and plotting of the data were performed using GraphPad Prism 6.0 and Microsoft Excel. NIH ImageJ was used for quantification of locomotion and fat analyses.

ACKNOWLEDGMENTS. We are grateful to Micah Belew, Yong-hak Seo, Griffin Walker, David Hoaglin, Eun-soo Kwon, Ashlyn Ritter, Silvia Corvera, Claire Bernard, Michael Czech, Victor Ambros, Michelle Mondoux, and Sri Devi Narasimhan for advice and discussion; Michelle Mondoux and Griffin Walker for defining gerospan; and Nina Bhabhalia for technical support. Some of the strains were kindly provided by the *Caenorhabditis* Genetics Center, which is funded by the NIH Office of Research Infrastructure Programs (P40 OD010440). This project was funded in part by grants from the National Institute of Aging (AG025891) and an endowment from the William Randolph Hearst Foundation. H.A.T. is a William Randolph Hearst Investigator.

- World Health Organization (2014) *10 Facts on Ageing and the Life Course*. Available at www.who.int/features/factfiles/ageing/en. Accessed November 28, 2014.
- Meara E, White C, Cutler DM (2004) Trends in medical spending by age, 1963–2000. *Health Aff (Millwood)* 23(4):176–183.
- Christensen K, Doblhammer G, Rau R, Vaupel JW (2009) Ageing populations: The challenges ahead. *Lancet* 374(9696):1196–1208.
- Narasimhan SD, Mukhopadhyay A, Tissenbaum HA (2009) InAKTivation of insulin/IGF-1 signaling by dephosphorylation. *Cell Cycle* 8(23):3878–3884.

- Smith ED, et al. (2008) Age- and calorie-independent life span extension from dietary restriction by bacterial deprivation in *Caenorhabditis elegans*. *BMC Dev Biol* 8:49.
- Kenyon C, Chang J, Gensch E, Rudner A, Tabtiang R (1993) A *C. elegans* mutant that lives twice as long as wild type. *Nature* 366(6454):461–464.
- Lakowski B, Hekimi S (1996) Determination of life-span in *Caenorhabditis elegans* by four clock genes. *Science* 272(5264):1010–1013.
- Felkai S, et al. (1999) CLK-1 controls respiration, behavior and aging in the nematode *Caenorhabditis elegans*. *EMBO J* 18(7):1783–1792.

9. Syntichaki P, Troulinaki K, Tavernarakis N (2007) eIF4E function in somatic cells modulates ageing in *Caenorhabditis elegans*. *Nature* 445(7130):922–926.
10. Pan KZ, et al. (2007) Inhibition of mRNA translation extends lifespan in *Caenorhabditis elegans*. *Aging Cell* 6(11):111–119.
11. Hansen M, et al. (2007) Lifespan extension by conditions that inhibit translation in *Caenorhabditis elegans*. *Aging Cell* 6(1):95–110.
12. Braeckman BP, Houthoofd K, Vanfleteren JR (2001) Insulin-like signaling, metabolism, stress resistance and aging in *Caenorhabditis elegans*. *Mech Ageing Dev* 122(7):673–693.
13. Murakami S, Johnson TE (1996) A genetic pathway conferring life extension and resistance to UV stress in *Caenorhabditis elegans*. *Genetics* 143(3):1207–1218.
14. Honda Y, Honda S (2002) Oxidative stress and life span determination in the nematode *Caenorhabditis elegans*. *Ann N Y Acad Sci* 959:466–474.
15. Lithgow GJ, White TM, Melov S, Johnson TE (1995) Thermotolerance and extended life-span conferred by single-gene mutations and induced by thermal stress. *Proc Natl Acad Sci USA* 92(16):7540–7544.
16. Lin YJ, Seroude L, Benzer S (1998) Extended life-span and stress resistance in the *Drosophila* mutant methuselah. *Science* 282(5390):943–946.
17. Kapahi P, Boulton ME, Kirkwood TB (1999) Positive correlation between mammalian life span and cellular resistance to stress. *Free Radic Biol Med* 26(5-6):495–500.
18. Bolanowski MA, Russell RL, Jacobson LA (1981) Quantitative measures of aging in the nematode *Caenorhabditis elegans*. I. Population and longitudinal studies of two behavioral parameters. *Mech Ageing Dev* 15(3):279–295.
19. Huang C, Xiong C, Kornfeld K (2004) Measurements of age-related changes of physiological processes that predict lifespan of *Caenorhabditis elegans*. *Proc Natl Acad Sci USA* 101(21):8084–8089.
20. Vellai T, McCulloch D, Gems D, Kovács AL (2006) Effects of sex and insulin/insulin-like growth factor-1 signaling on performance in an associative learning paradigm in *Caenorhabditis elegans*. *Genetics* 174(1):309–316.
21. Murakami H, Bessinger K, Hellmann J, Murakami S (2005) Aging-dependent and -independent modulation of associative learning behavior by insulin/insulin-like growth factor-1 signal in *Caenorhabditis elegans*. *J Neurosci* 25(47):10894–10904.
22. Burger JM, Buechel SD, Kaweckii TJ (2010) Dietary restriction affects lifespan but not cognitive aging in *Drosophila melanogaster*. *Aging Cell* 9(3):327–335.
23. Burger JM, Hwangbo DS, Corby-Harris V, Promislow DE (2007) The functional costs and benefits of dietary restriction in *Drosophila*. *Aging Cell* 6(1):63–71.
24. Avanesian A, Khodayari B, Felgner JS, Jafari M (2010) Lamotrigine extends lifespan but compromises health span in *Drosophila melanogaster*. *Biogerontology* 11(1):45–52.
25. Rockwood K, et al. (2005) A global clinical measure of fitness and frailty in elderly people. *CMAJ* 173(5):489–495.
26. Peña FG, et al. (2014) Comparison of alternate scoring of variables on the performance of the frailty index. *BMC Geriatr* 14:25.
27. Herndon LA, et al. (2002) Stochastic and genetic factors influence tissue-specific decline in ageing *C. elegans*. *Nature* 419(6909):808–814.
28. Collins JJ, Huang C, Hughes S, Kornfeld K (December 7, 2007) The measurement and analysis of age-related changes in *Caenorhabditis elegans*. *WormBook*, ed The *C. elegans* Research Community, 10.1895/wormbook.1.137.1. Available at www.wormbook.org. Accessed November 28, 2014.
29. Gerstbrein B, Stamatias G, Kollias N, Driscoll M (2005) In vivo spectrofluorimetry reveals endogenous biomarkers that report healthspan and dietary restriction in *Caenorhabditis elegans*. *Aging Cell* 4(3):127–137.
30. Ibáñez-Ventoso C, Driscoll M (2009) MicroRNAs in *C. elegans* aging: Molecular insurance for robustness? *Curr Genomics* 10(3):144–153.
31. Iwasa H, Yu S, Xue J, Driscoll M (2010) Novel EGF pathway regulators modulate *C. elegans* healthspan and lifespan via EGF receptor, PLC-gamma, and IP3R activation. *Aging Cell* 9(4):490–505.
32. Leiser SF, Begun A, Kaerberlein M (2011) HIF-1 modulates longevity and healthspan in a temperature-dependent manner. *Aging Cell* 10(2):318–326.
33. Onken B, Driscoll M (2010) Metformin induces a dietary restriction-like state and the oxidative stress response to extend *C. elegans* healthspan via AMPK, LKB1, and SKN-1. *PLoS ONE* 5(1):e8758.
34. Weindruch R, Walford RL, Fligiel S, Guthrie D (1986) The retardation of aging in mice by dietary restriction: Longevity, cancer, immunity and lifetime energy intake. *J Nutr* 116(4):641–654.
35. Bordone L, Guarente L (2005) Calorie restriction, SIRT1 and metabolism: Understanding longevity. *Nat Rev Mol Cell Biol* 6(4):298–305.
36. Partridge L, Piper MD, Mair W (2005) Dietary restriction in *Drosophila*. *Mech Ageing Dev* 126(9):938–950.
37. Greer EL, Brunet A (2009) Different dietary restriction regimens extend lifespan by both independent and overlapping genetic pathways in *C. elegans*. *Aging Cell* 8(2):113–127.
38. McKay JP, Raizen DM, Gottschalk A, Schafer WR, Avery L (2004) eat-2 and eat-18 are required for nicotinic neurotransmission in the *Caenorhabditis elegans* pharynx. *Genetics* 166(1):161–169.
39. Liu X, et al. (2005) Evolutionary conservation of the clk-1-dependent mechanism of longevity: Loss of mclk1 increases cellular fitness and lifespan in mice. *Genes Dev* 19(20):2424–2434.
40. Gingras AC, Raught B, Sonenberg N (1999) eIF4 initiation factors: Effectors of mRNA recruitment to ribosomes and regulators of translation. *Annu Rev Biochem* 68:913–963.
41. Harrison DE, et al. (2009) Rapamycin fed late in life extends lifespan in genetically heterogeneous mice. *Nature* 460(7253):392–395.
42. Yen K, Steinsaltz D, Mobbs CV (2008) Validated analysis of mortality rates demonstrates distinct genetic mechanisms that influence lifespan. *Exp Gerontol* 43(12):1044–1051.
43. Clegg A, Young J, Iliffe S, Rikkert MO, Rockwood K (2013) Frailty in elderly people. *Lancet* 381(9868):752–762.
44. Lithgow GJ, White TM, Hinerfeld DA, Johnson TE (1994) Thermotolerance of a long-lived mutant of *Caenorhabditis elegans*. *J Gerontol* 49(6):B270–B276.
45. Metter EJ, Talbot LA, Schrager M, Conwit R (2002) Skeletal muscle strength as a predictor of all-cause mortality in healthy men. *J Gerontol A Biol Sci Med Sci* 57(10):B359–B365.
46. Fisher AL (2004) Of worms and women: Sarcopenia and its role in disability and mortality. *J Am Geriatr Soc* 52(7):1185–1190.
47. Glenn CF, et al. (2004) Behavioral deficits during early stages of aging in *Caenorhabditis elegans* result from locomotory deficits possibly linked to muscle frailty. *J Gerontol A Biol Sci Med Sci* 59(12):1251–1260.
48. Chow DK, Glenn CF, Johnston JL, Goldberg IG, Wolkow CA (2006) Sarcopenia in the *Caenorhabditis elegans* pharynx correlates with muscle contraction rate over lifespan. *Exp Gerontol* 41(3):252–260.
49. Pan CL, Peng CY, Chen CH, McIntire S (2011) Genetic analysis of age-dependent defects of the *Caenorhabditis elegans* touch receptor neurons. *Proc Natl Acad Sci USA* 108(22):9274–9279.
50. Tank EM, Rodgers KE, Kenyon C (2011) Spontaneous age-related neurite branching in *Caenorhabditis elegans*. *J Neurosci* 31(25):9279–9288.
51. Liu J, et al. (2013) Functional aging in the nervous system contributes to age-dependent motor activity decline in *C. elegans*. *Cell Metab* 18(3):392–402.
52. Shaham S, ed (January 2, 2006) *WormBook: Methods in cell biology*. *WormBook*, ed The *C. elegans* Research Community, 10.1895/wormbook.1.49.1. Available at www.wormbook.org. Accessed November 28, 2014.
53. Avery L, Shtonda BB (2003) Food transport in the *C. elegans* pharynx. *J Exp Biol* 206(Pt 14):2441–2457.
54. Jung T, Bader N, Grune T (2007) Lipofuscin: Formation, distribution, and metabolic consequences. *Ann N Y Acad Sci* 1119:97–111.
55. McColl G, Jenkins NL, Walker DW, Lithgow GJ (2000) Testing evolutionary theories of aging. *Ann N Y Acad Sci* 908:319–320.
56. Jenkins NL, McColl G, Lithgow GJ (2004) Fitness cost of extended lifespan in *Caenorhabditis elegans*. *Proc Biol Sci* 271(1556):2523–2526.
57. Wong A, Boutis P, Hekimi S (1995) Mutations in the clk-1 gene of *Caenorhabditis elegans* affect developmental and behavioral timing. *Genetics* 139(3):1247–1259.
58. Gems D, et al. (1998) Two pleiotropic classes of daf-2 mutation affect larval arrest, adult behavior, reproduction and longevity in *Caenorhabditis elegans*. *Genetics* 150(1):129–155.
59. Crawford D, Libina N, Kenyon C (2007) *Caenorhabditis elegans* integrates food and reproductive signals in lifespan determination. *Aging Cell* 6(5):715–721.
60. Song A, et al. (2010) A *C. elegans* eIF4E-family member upregulates translation at elevated temperatures of mRNAs encoding MSH-5 and other meiotic crossover proteins. *J Cell Sci* 123(Pt 13):2228–2237.
61. Arantes-Oliveira N, Berman JR, Kenyon C (2003) Healthy animals with extreme longevity. *Science* 302(5645):611.
62. Chen D, et al. (2013) Germline signaling mediates the synergistically prolonged longevity produced by double mutations in daf-2 and rsk-1 in *C. elegans*. *Cell Rep* 5(6):1600–1610.
63. Partridge L, Gems D, Withers DJ (2005) Sex and death: What is the connection? *Cell* 120(4):461–472.
64. Longo VD, Finch CE (2003) Evolutionary medicine: From dwarf model systems to healthy centenarians? *Science* 299(5611):1342–1346.
65. Stiernagle T (2006) Maintenance of *C. elegans*. *WormBook*, ed The *C. elegans* Research Community, 10.1895/wormbook.1.101.1. Available at www.wormbook.org. Accessed November 28, 2014.
66. Costa M, Draper BW, Priess JR (1997) The role of actin filaments in patterning the *Caenorhabditis elegans* cuticle. *Dev Biol* 184(2):373–384.
67. Yen K, et al. (2010) A comparative study of fat storage quantitation in nematode *Caenorhabditis elegans* using label and label-free methods. *PLoS ONE* 5(9):e12810.
68. Van Rompaye B, Jaffar S, Goetghebeur E (2012) Estimation with Cox models: Cause-specific survival analysis with misclassified cause of failure. *Epidemiology* 23(2):194–202.